JASMAC
Conference of the Japan Society of Microgravity Appllication
JASMA

OR-0713

月資源レーザー還元法におけるレーザー照射アルミナ表面でのアルミニウム粒子生成

Aluminum Particle Production on Laser-ablated Alumina in Laser Reduction Method for Utilization of Lunar Resources

○田中聖也[1]，田中直輝[1]，小紫公也[1]，小泉宏之[2]

○**Seiya TANAKA[1], Naoki TANAKA[1], Kimiya KOMURASAKI[1], and Hiroyuki KOIZUMI[2]**

1　東京大学大学院工学系研究科，School of Engineering, the University of Tokyo,
2　東京大学大学院新領域創成科学研究科，Graduate School of Frontier Science, the University of Tokyo.

1. Introduction

The utilization of lunar resources has been proposed for manned moon exploration[1]. The lunar surface is covered with regolith, whose composition is like that of Earth, and alumina (Al_2O_3) accounts for 32% of regolith at lunar highland[2]. Aluminum, which is obtained by reducing alumina, is one of the most useful materials for the construction of a moon base due to its excellent cold-resistance mechanical properties[3]. However, the only practical alumina reduction method in use, the Hall-Heroit method, has the problem of consuming carbon as a reducing agent that cannot be mined on the moon[4]. A molten salt electrolysis method using an inert anode has been studied to establish a carbon-free electrolysis method[5]. However, due to the low current efficiency, energy consumption was much greater than the value in practical methods.

The laser ablation method has been researching for carbon-free alumina reduction[6]. By the laser irradiation, the alumina is heated to the temperature over the boiling point of alumina and ejects an ablation plume, consisting of Al, O, O_2, AlO, AlO_2 and Al_2O_2. Ejected aluminum in the ablation plume is cooled down and expected to adhere to a collecting plate. However aluminum adhesion was not observed on the plate even though the existence of aluminum atoms in vaporized alumina gas was confirmed by emission spectroscopy. On the other hand, the formation of aluminum on the surface of the laser-ablated alumina rod was confirmed by the method based on JIS H 8672: inserting the laser-ablated alumina rod into sodium hydrogen solution and checking hydrogen bubble eruption caused by the chemical reaction of aluminum and sodium hydrogen. The observed violent bubble eruption implies more aluminum particle production than expected.

The heterogeneous nucleation theory is one of the applicable theories for this aluminum particle production. The nucleation and its growth are determined by the Gibbs free energy calculated from volume free energy and interfacial energy. The critical radius for nucleation in the aluminum particle production, the minimum particle size for thermodynamically stable, is calculated from Eq. (1), where the Gibbs free energy becomes maximum.

$$r_p^* = \frac{2\sigma}{\rho_{Al} R T \ln\left(\frac{P_{Al}}{P_s(T_{rod})}\right)} \quad (1)$$

r_p^* represents the critical radius for nucleation, σ denotes the surface tension, ρ_{Al} is the density of liquid aluminum, R is gas constant, T and T_{rod} stands for the gas temperature and the alumina rod surface temperature respectively, and P_{Al} and P_s means the partial pressure and the saturated vapor pressure of aluminum. By substituting the representative value of P_{Al}/P_s (T_{rod}) = 1.0, σ = 0.8 N/m, ρ_{Al} = 2100 kg/m^3, R = 300 J/kg K, and T = 2300 K to Eq. (1), the critical radius for nucleation

was calculated to r_p*= 0.1 μm. Therefore, the radius of aluminum particles on the rod surface should be larger than the 0.1 μm, if this aluminum particle production is consistent with this theory.

In this research, the presence of aluminum particles were verified on the laser-ablated alumina rod surface by the observation with scanning electron microscope (SEM) and chemical composition measuremtn with energy dispersive X-ray spectroscopy (EDX). Moreover, the radius of aluminum particles was measured to verify whether the heterogeneous nucleation theory can be applied. By using the measured radius, the mass of the produced aluminum was estimated to judge whether this aluminum particle production would be the aluminum collection way in the alumina reduction. From the results, the formation mechanism of aluminum particle would be discussed, and the knowledge for an efficient aluminum collection system would be obtained.

2. Experimental setup

2.1 Laser ablation of alumina using a continuous-wave CO_2 laser

A schematic of the laser ablation system is presented in Fig. 1. A 4-mm diameter sintered alumina rod was inserted into a rod holder in the test chamber. The sintered alumina rod was irradiated with a continuous-wave CO_2 laser (wavelength 10.6 μm) with a power of 0.40–2.0 kW through a convex lens for 1.0 sec. The focal length of the lens was 210 mm, and the laser spot size on the rod surface was 0.49 mm. At first, the chamber was evacuated to 50 Pa using a rotary pump. The chamber was supplied with argon gas at a mass flow rate of 6.0 slm, and the atmospheric pressure in the chamber was kept at 1.0 atm during the laser irradiation. This experiment was performed three times for each laser power condition.

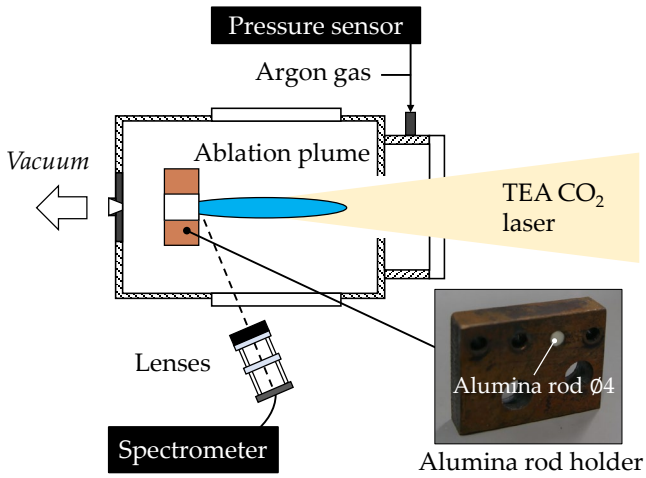

Fig. 1 Alumina laser ablation system using the plate-shaped holder.

2.2 Aluminum detection on alumina rod surface

After the laser irradiation was completed, the state of the ablated alumina rod surface was observed by SEM (JEOL, JEM IT-100). For each alumina rod, twelve SEM photographs were taken from the center to the edge of the rod surface. A qualitative analysis of EDX measured the molar fraction (Al:O) of the rod surface. Besides, elemental identification was performed using a sodium hydrogen solution to detect aluminum on the rod surface. The alumina rods after laser ablation were inserted into a flask containing 3.0 mol/L NaOH solution for 30 min. The temperature of the solution was maintained at 90 °C with a heater to facilitate the chemical reaction. Among the expected materials, only aluminum can generate hydrogen. After this chemical reaction process, SEM observation of the rod surface was performed. From the SEM photographs, rod surface coverage and mean particle radius of particles were measured using Python and ImageJ to calculate the mass of produced aluminum.

3. Result and discussion

3.1 SEM observation of alumina rod surface after laser ablation

Fig. **2** presents an overall view of ablated alumina rod and SEM pictures of the alumina rod surface at a laser power of

2.0 kW. Spherical particles were present on the molten-solidified surface, as shown in Fig. 2. This result suggests that the particles were formed during the cooling process of the rods after laser ablation at temperatures below the melting point of alumina. The distribution of produced particles was axisymmetric and changed according to the radial position on the rod surface. At the inner part of the rod surface, many particles were densely aligned on the grain boundaries. Considering the heterogeneous nucleation theory, these aligned particles should be caused by the surface energy at the grain boundaries. On the surface around the rod edge, the particles were uniformly present. These different distributions of particles could be produced by the cooling rate of alumina rod surface.

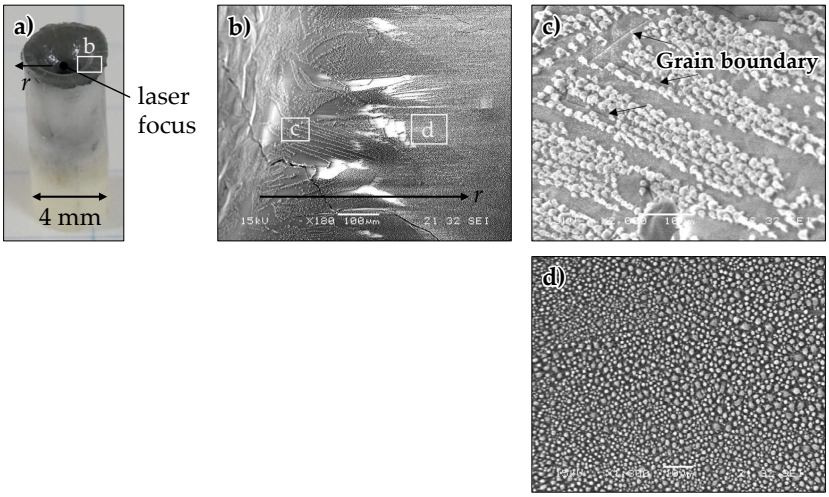

Fig. 2 Photograph and SEM pictures of a hollowed-out alumina rod surface at a laser power of 2.0 kW: a) an overall view of alumina rod after laser ablation, b) the rod surface (×100), c) the inner part of rod surface (×2000), and d) the surface around the rod edge (×1300).

3.2 Aluminum detection on alumina rod surface

The analysis result of EDX showed the molar ratio of particles was $Al_2O_{1.1–1.2}$ regardless of its position on the rod surface. Yanagida et al. has shown computationally that oxygen-deficient alumina with a lower molar ratio of oxygen than $Al_2O_{2.3}$ cannot exist [7]. Therefore, the particles of $Al_2O_{1.1–1.2}$ were aluminum with an oxide film. Unlike the chemical composition of particles, the molar ratio of the rod surface was $Al_2O_{2.3–2.4}$; oxygen-deficient alumina.

SEM observation of the alumina rod surface after the chemical reaction with NaOH solution showed that the interior of the particle was removed due to the chemical reaction, and the oxide film was left. In addition to the EDX result, the SEM observation indicates the inner of the particles were aluminum. The thickness of the oxide film measured from the SEM photographs was 0.1-0.2 μm.

3.3 Image analysis of aluminum particles in SEM pictures

The measurements of rod surface coverage and mean particle radius are shown in Fig. 3. The particle distribution and radius varied with the radial position of the alumina rod surface, and both the coverage and particle radius increased with the laser power. The mean particle radius was varied from 0.13 μm to 1.7 μm. Considering the thickness of an oxide film, the minimum radius of observed aluminum particles was 0.11 μm, which is larger than the critical radius for aluminum nucleation: r_p*= 0.1 μm. Therefore, this aluminum particle production is consistent with the heterogeneous nucleation theory. The rod surface coverage essentially increased with distance from the rod center. At laser powers of 0.40 and 1.0 kW, the coverage was zero because no particles were present near the edge of the rod surface without melting. Furthermore, contrary to the trend of distance from the center of the rod, large coverage was observed at 0.40 kW and 2.0 kW with r = 0.23 and r = 0.54–0.70 mm, respectively.

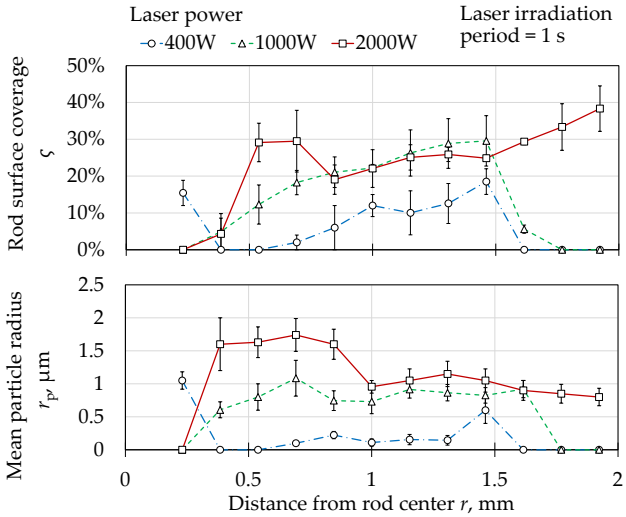

Fig. 3 Measured rod surface coverage and mean particle radius of particles vs. distance from the rod center at various laser powers.

3.4 Mass calculation of produced aluminum particles

The number density of aluminum particles on the rod surface was calculated in each SEM photographs from the measured rod surface coverage and mean particle radius. By using the measured mean particle radius, oxide film thickness, and the calculated number density, the mass of aluminum produced on the alumina rod surface was calculated. The calculation results show the mass of produced aluminum particles was 0.016 mg at a laser power of 2.0 kW, and the energy consumption for aluminum production was 91 MWh/kg-Al, which was three orders of magnitude larger than the electrolysis method. Therefore, this aluminum particle production was not enough for the aluminum collection method in laser ablation. An improved aluminum collection method based on the aluminum particle production mechanism should be developed.

3.5 Discussion on mechanisms of aluminum particle production

The mechanisms of aluminum particle production should be elucidated for an efficient aluminum collection method. Two mechanisms could be proposed for the aluminum particle production on the alumina rod surface after laser ablation . One is the vapor deposition from Al-O gas. After the laser irradiation, the vaporized and dissociated alumina gas containing aluminum atoms existed above the alumina rod surface. By cooling down the gas in contact with the rod surface, the aluminum can adhere to the alumina rod. The other mechanism is impurity precipitation from the laser-ablated alumina rod. In the cooling process of a mixture, a rapid cooling causes the impurity precipitation because a lattice formation rate of base material overcomes a diffusion velocity of atoms. Therefore, in the case of a large cooling rate of alumina rod surface, aluminum can precipitate from the laser-ablated alumina rod with low oxygen deficiency.

Aluminum nucleation in both mechanisms are determined from the heterogeneous nucleation theory, and the time history of alumina rod temperature would be an important factor for the mass of produced aluminum. For realizing the efficient aluminum collection in the laser ablation method, the effects of alumina cooling rate and alumina rod temperature should be clarified experimentally.

4. Conclusion

We verified the presence of aluminum particles from the SEM observation with EDX analysis and chemical reaction with the sodium hydroxide solution. Conclusions obtained from this research are summarized as presented below.

1. Spherical aluminum particles with an oxide film were produced on the alumina rod surface after the laser ablation in the rod cooling process. The minimum aluminum particle radius was 0.11 μm, which was larger than the critical radius for aluminum nucleation, and this result indicated that the aluminum particle production on the rod surface could be discussed from the heterogeneous nucleation theory.

2. The aluminum particle production mass at a laser power of 2.0 kW was 0.016 mg, and the energy consumption for aluminum particle production was 91 MWh/kg-Al, which was three orders of magnitude larger than the electrolysis method. The mechanism of aluminum particle production on rod surface and effects of alumina rod cooling rate and rod surface temperature should be elucidated for further improvement of the aluminum collection in laser ablation.

Acknowledgment

This work was supported by Japan EXpert Clone Corporation and Japan Society for the Promotion of Science KAKENHI Grant Number JP20K20542. The use of the facilities of the Institute for Solid State Physics, the University of Tokyo, is gratefully acknowledged.

References

1) Anand, M., Crawford, I. A., Balat-Pichelin, M., Abanades, S., Westrenen, W. van, Peraudeau, G., Jaumann, R., and Seboldt, W., "A brief review of chemical and mineralogical resources on the Moon and likely initial in situ resource utilization (ISRU) applications," Planetary and Space Science, **74** (2012) 42–48.
2) Heiken, G. H., Vaniman, D. T., and French, B. M., "Lunar Sourcebook," Cambridge University Press, (1991) 357–371.
3) Blinova, A.V., Chekmareva, P. P., Il'ichev, V. Ya., and Telegon, A. I., "Mechanical Properties of Aluminum Alloys at Temperatures Down to 4.2 K," Metal science and heat treatment, **17** (1975) 502–505.
4) Masuko, N., and Masio, K., "Present aluminum smelting technology," Journal of the Japan Institute of Light Metals, **65** (2015) 66–71.
5) Xie, K., Shi, Z., Xu, J., Hu, X., Gao, B., and Wang, Z., "Aluminothermic Reduction-Molten Salt Electrolysis Using Inert Anode for Oxygen and Al-Base Alloy Extraction from Lunar Soil Simulant," Journal of Metals, **89** (2017) 1963–1969.
6) Tanaka, S., Yamada, S., Soga, R., Komurasaki, K., Kawashima, R., and Koizumi, H., "Alumina reduction by laser ablation using a continuous-wave CO2 laser toward lunar resource utilization," Vacuum, **167** (2018) 495–499.
7) Yanagida, H., and Kroger, F. A., "The Sytem Al-O," Journal of The American Ceramic Society, **51** (1968) 700–706.